Zr-TUD-1: A novel heterogeneous catalyst for the Meerwein–Ponndorf–Verley reaction

Anand Ramanathan [a,b], Dirk Klomp [a], Joop A. Peters [a], Ulf Hanefeld [a,*]

[a] *Gebouw voor Scheikunde, Technische Universiteit Delft, Julianalaan 136, 2628 BL Delft, The Netherlands*
[b] *Advanced Chemical Technology Division, Korea Research Institute of Chemical Technology (KRICT), P.O. Box 107, Yusung, Daejeon 305-600, Republic of Korea*

Abstract

A new, three-dimensional, amorphous mesoporous silicate containing zirconium, Zr-TUD-1, was synthesised via a direct hydrothermal treatment method using triethanolamine as the template. The mesoporosity of Zr-TUD-1 was confirmed by XRD, N_2 sorption and HR-TEM studies. The acid sites present in Zr-TUD-1 were evaluated by FT-IR studies of pyridine adsorption and shown to be predominately Lewis acidic. The nature of zirconium in Zr-TUD-1 was established by FT-IR, XPS and UV–vis studies. Zr-TUD-1 was tested in the Meerwein–Ponndorf–Verley reduction. It showed a promising activity, in particular for the stereoselective reduction of steroids.
© 2006 Elsevier B.V. All rights reserved.

*Keywords:* Mesoporous silica; Meerwein–Ponndorf–Verley; Prins-reaction; Zirconium

1. Introduction

The Meerwein–Ponndorf–Verley reduction and its counterpart, the Oppenauer oxidation are well-established, mild redox reactions [1,2]. Its high selectivity has made it particularly popular in steroid chemistry, allowing efficient reductions even on an industrial scale. They are commonly catalysed by equimolar amounts of aluminium(III) isopropoxide, however more recently the catalytic application of bis(dialkoxyaluminium) complexes [3,4] or aluminium(III) isopropoxide [5], zirconium(IV) isopropoxide [6,7] and lanthanide isopropoxides [8–10] have been described. A significant step forward was the introduction of the heterogeneous catalysts for this reaction, such as metal oxides [11], hydrous zirconia [12], hydrotalcites [13,14] and zeolite H-beta [15,16], recently they were followed by the very active Al-free Sn-beta [17] and Al-free Zr-beta [18–20]. The mechanisms of the homogeneous and heterogeneous reaction have been elucidated. The reactions were proven to proceed via a carbon to carbon hydrogen transfer reaction, while the

Lewis acid catalyses and coordinates this process (Scheme 1) [21,22].

Drawbacks of the Al-free Sn and Zr substituted beta zeolites are their limited pore size and their complex synthesis. Similarly, the grafting of zironcium(IV) propoxide onto MCM-41, MCM-48 and SBA-15 is labour intensive [23]. A less labor intensive preparation of zirconium containing mesoporous silicate yields a material with a one-dimensional pore structure, which limits diffusion [24]. In contrast, it was recently demonstrated that the three-dimensional, mesoporous silicate TUD-1 [25] can readily be prepared with isolated metals incorporated into the framework, such as Al, Co, Cu, Fe and Ti [26–31]. The templating method applied for the synthesis of TUD-1 uses triethanolamine, which acts both as template in the mesopore formation and as a metal complexing agent. This has the advantage that the metal is deposited on the surfaces of the mesopores [31]. Utilising zirconium(IV) propoxide as metal source with triethanolamine as template in a one-pot surfactant-free procedure based on the sol–gel technique, Zr-TUD-1 with a Si/Zr ratio of 25 was readily prepared. Zirconium was the metal of choice, since it is tetrahedrally coordinated and was shown to be particularly active in the Meerwein–Ponndorf–Verley reaction when incorporated into Al-free zeolite beta [18–20]. In addition the pores of TUD-1 are large enough to accommodate steroids

* Corresponding author. Tel.: +31 15 278 9304; fax: +31 15 278 1415.
E-mail addresses: anand_ncl@yahoo.com (A. Ramanathan),
u.hanefeld@tudelft.nl (U. Hanefeld).
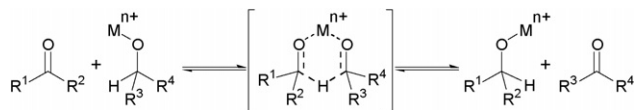
Scheme 1. Mechanism of the Meerwein–Ponndorf–Verley reduction and Oppenauer oxidation.

such as cholesterol, that cannot enter the pores of zeolite H-beta [32].

In this paper, we report the direct hydrothermal, cost-effective synthesis of zirconium containing 3D-mesoporous silica Zr-TUD-1 with a Si/Zr ratio of 25 and its application as catalyst in the Meerwein–Ponndorf–Verley reaction.

2. Experimental

2.1. Chemicals

All chemicals were purchased from Aldrich, Janssen or Acros. In the synthesis of the Zr-TUD-1 the chemicals were used as received. For the catalysis experiments, the anhydrous solvents and solids were used as received, liquids were dried and distilled prior to use and Zr-TUD-1 was activated in the presence of air at up to 600 °C at a temperature ramp of 1 °C/min and subsequent heating at 600 °C for 10 h. These experiments were performed in dried glassware under a nitrogen atmosphere.

2.2. Synthesis of Zr-TUD-1 (Si/Zr = 25)

Tetraethyl orthosilicate (98%, 33.8 g) was added to a mixture of zirconium(IV) propoxide (70 wt.% in 1-propanol, 2.98 g) and 2-propanol (25 mL). After stirring for a few minutes, a mixture of triethanolamine (97%, 24.5 g) and water (18.5 mL) was added followed by addition of a tetraethylammonium hydroxide solution (35 wt.%, 20.1 g) under vigorous stirring. The clear gel obtained after these steps was then aged at room temperature for 12–24 h, dried at 98 °C for 12–24 h, followed by hydrothermal treatment in a Teflon lined autoclave at 180 °C for 4–24 h and finally calcined in the presence of air at up to 600 °C at a temperature ramp of 1 °C/min and subsequent heating at 600 °C for 10 h. The Zr-TUD-1 obtained could be used for catalysis immediately or was, upon standing for a prolonged period of time, reactivated by repeating the calcination procedure.

2.3. Characterization

For the elemental analysis of Si and Zr, the samples were dissolved in an aqueous solution of 1% HF and 1.3% H_2SO_4. The resulting solution was measured with inductively coupled plasma-optical emission spectroscopy (ICP-OES) on a Perkin-Elmer Optima 3000DV instrument. Powder XRD patterns were obtained on a Philips PW 1840 diffractometer equipped with a graphite monochromator using Cu Kα radiation. The textural parameters were evaluated from volumetric nitrogen physisorption at 77 K on a Quantachrome Autosorb-6B instrument. Transmission electron microscopy (TEM) was performed using a Philips CM30T electron microscope with a LaB6 filament as

the source of electrons operated at 300 kV. UV–vis spectra were collected at room temperature on a Shimadzu UV-2450 spectrophotometer using $BaSO_4$ as reference.

FT-IR spectra of self-supported wafers and KBr diluted wafers of Zr-TUD-1 samples were recorded using a Nicolet AVATAR 360 FT-IR instrument. Acid strength distribution was evaluated by contacting pyridine vapours (20 Torr) for 30 min at 100 °C on self-supported wafers of Zr-TUD-1 (15–25 mg/cm^2) after evacuation (500 °C, 2 h, 10 Pa) in a custom made vacuum cell with CaF_2 windows. The physisorbed pyridine was subsequently removed by evacuation at 150 °C for 30 min. The spectra were recorded at room temperature with a resolution of 2 cm^{-1} averaging over 500 scans after desorbing pyridine at 200 °C.

The XPS measurements were performed with a PHI 5400 ESCA provided with a dual Mg/Al anode X-ray source, a hemispherical capacitor analyser and a 5 keV ion-gun. All spectra were recorded with unmonochromated magnesium radiation. The X-ray source was operated at an acceleration voltage of 15 kV and power of 400 W. The spectra of the separate photoelectron and Si-Auger electron lines were recorded with a pass energy of 35.75 eV and a step size of 0.2 eV. The Zr-Auger electron line was recorded with a pass energy of 89.45 eV and a step size of 0.5 eV. The spectra were evaluated with Multipak 6.1A software (Physical Electronics).

2.4. General procedure for the Meerwein–Ponndorf–Verley reductions

All experiments were performed in dried glassware under a nitrogen atmosphere. Zr-TUD-1 (50 mg) was introduced into a Schlenk flask. Isopropanol (4 mL) was added followed by 1,3,5-triisopropylbenzene (0.1 mL) and the ketone or aldehyde (2 mmol). The mixture was heated to 80 °C and the reaction was followed by taking small samples, these were analysed as described below. The experiments with Al-TUD-1 (Si/Al = 25) and H-beta (Si/Al = 25) were performed analogously, also using 50 mg of the solid catalyst.

2.5. Analysis

NMR spectra were recorded on a Varian Unity Inova-300 spectrometer at 25 °C. Mass spectra were recorded with a VG SE spectrometer at 70 eV. Reactions were followed by gas chromatography by using a Shimadzu GC-17A gas chromatograph, equipped with a 25 m × 0.32 mm chiral column Chrompack^{TM} Chirasil-Dex CB, split injector (1/97) at 220 °C, a Flame Ionisation Detector at 220 °C and He as carrier gas. Retention times (min) at 120 °C isotherm: 1,3,5-triisopropylbenzene (internal standard) (4.0), 4-*tert*-butyl cyclohexanone (**1**) (4.7), 4-(*trans*)-*tert*-butyl cyclohexanol (**3**) (5.6), 4-(*cis*)-*tert*-butyl cyclohexanol (**2**) (5.9), acetophenone (**4**) (1.7), (*S*)-1-phenylethanol ((*S*)-**5**) (3.4), (*R*)-1-phenylethanol ((*R*)-**5**) (3.7), cyclohexyl methyl ketone (**6**) (1.6), (*S*)-1-cyclohexyl ethanol ((*S*)-**7**) (2.70), (*R*)-1-cyclohexyl ethanol ((*R*)-**7**) (2.75), cyclohex-2-enone (**8**) (1.2), (*S*)-cyclohex-2-enol ((*S*)-**9**) (1.52), (*R*)-cyclohex-2-enol ((*R*)-**9**) (1.56), octanal (**10**) (0.9), 1-octanol (**11**) (1.0), 1,1-bis(octyloxy)octane (**12**) (1.4), 3-octanone (**13**) (0.8), 3-octanol
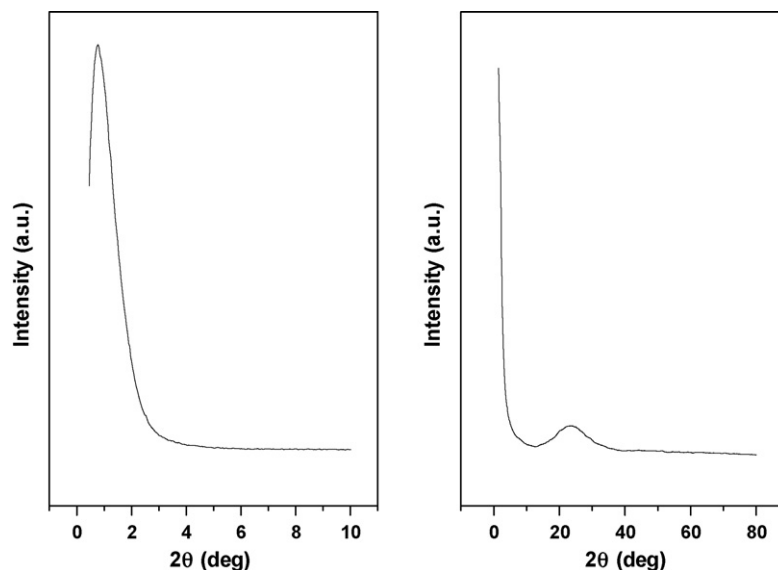
Fig. 1. XRD powder pattern of calcined Zr-TUD-1.

(**14**) (1.1), (*S*)-citronellal (**15**) (2.0), (*S*)-citronellol (4.1), (+)-isopulegol ((+)-**16**) (2.9), isomer(s) of (**16**) (3.6), cinnamaldehyde (**17**) (5.3), cinnamyl alcohol (**18**) (10.3). The structure of (+)-isopulegol ((+)-**16**) was confirmed by NMR spectroscopy. Direct comparison with a commercial sample of (−)-**16** (Janssen) by ^{1}H and ^{13}C NMR spectroscopy with a Varian Unity Inova-300 spectrometer at 25 °C revealed identical spectra. Conversions of the steroids oestrone (**19**) and 5α-cholestan-3-one (**21**) and α/β ratios of **20** and **22** were determined by integration after quantitative ^{13}C NMR spectroscopy with a Varian Unity Inova-300 spectrometer at 25 °C. In the case of **19** the signal for the carbonyl group (C-17 = 219.4 ppm) remained unchanged while no signals for the α- or β-alcohol **20** (α-C-17 = 77.91 ppm; β-C-17 = 79.96 ppm) were detected. The ^{13}C NMR spectrum of the reaction product **22** (reduction of **21**) showed no carbonyl resonance (C-3 of **21** = 212.1 ppm). Two sets of signals were observed, which could be assigned to α- and β-**22**. The molar ratios of these isomers was determined by integration of the resonances at 71.0 ppm (β-C-3 of **22**) and 66.2 ppm (α-C-3 of **22**) in a quantitative ^{13}C NMR spectrum [33].

3. Results and discussion

3.1. Zr-TUD-1 as novel mesoporous material

A broad peak at the low angle was observed in the X-ray powder diffraction pattern for calcined Zr-TUD-1 (Fig. 1), indicating a mesoporous and amorphous character of the material. No evidence of crystalline ZrO_2 was observed in the X-ray diffractograms, indicating that Zr is incorporated into the framework of TUD-1. The mesoporosity and amorphous character was also confirmed by transmission electron micrographs (Fig. 2), while the pores are clearly visible they are not ordered nor are ordered channels visible. Indeed, Fig. 2 shows a sponge-like 3D structure characteristic for TUD-1 mesoporous materials [25–31].

As expected no crystalline zirconia particles were observed. Zr-TUD-1 showed a type IV isotherm, pointed out by the large uptake of nitrogen at relative pressures between 0.5 and 0.9 p/p_0, due to capillary condensation in the mesopores (Fig. 3). It appears from the desorption data of Zr-TUD-1, as if the distribution is narrow but the adsorption data show a much broader distribution. This discrepancy is caused by networking effects, from which it can be concluded that the outside of the material is homogeneous, while larger pores or cavities exist inside the material. Physico-chemical properties of Zr-TUD-1 are listed in Table 1. The excellent correlation of the Si/Zr ratio in the synthesis gel with that in the product demonstrates the high predictability of the synthesis, as was also observed with other M-TUD-1 materials [28–30].

The observed binding energy of Zr $3d_{5/2}$ (183.2 eV), as determined by XPS measurements, is significantly higher than that of ZrO_2 (182.2 eV) and close to that of Zr in $ZrSiO_4$ (183.3 eV) [34]. Also the binding energies of O 1s were observed at 532.4 eV and they are significantly higher than that of ZrO_2 (530.2 eV) [34]. The binding energy values for Zr $3d_{5/2}$ and O 1s are similar to those observed for Zr in the MFI structure [35],
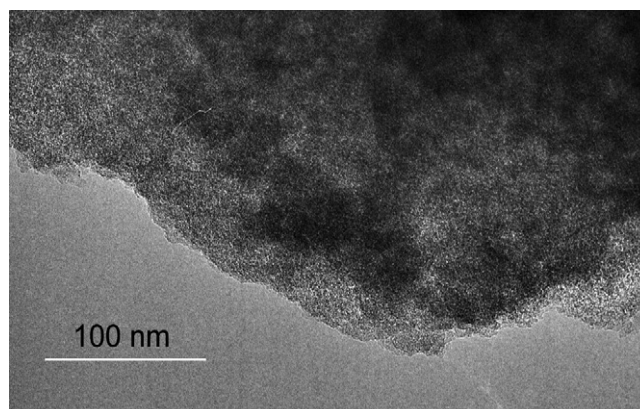

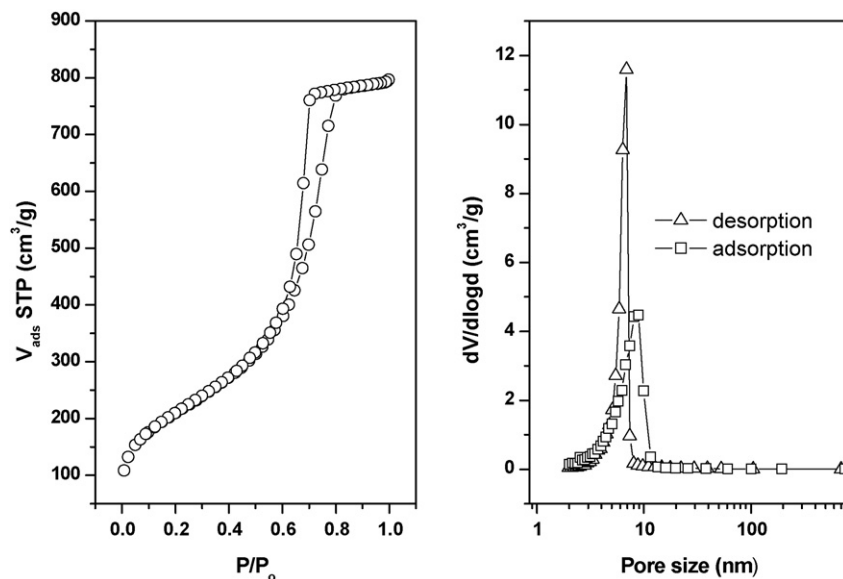Fig. 2. Transmission electron micrograph of calcined Zr-TUD-1.

Fig. 3. N_2 adsorption and desorption isotherms at 77 K and the corresponding pore size distribution of Zr-TUD-1.

Table 1
Physico-chemical characteristics of Zr-TUD-1

Sample	Zr-TUD-1
Si/Zr ratio in synthesis gel	25
Si/Zr ratio in the product[a]	25
BET surface area (m^2/g)	764
Pore volume (cm^3/g)	1.23
Pore diameter (nm)	6.9

[a] Determined by ICP.

zeolite beta [18–20] and mesoporous silicas [36]. These two observations are strong evidence for the presence of zirconium in the framework of TUD-1 matrix.

Diffuse reflectance UV–vis spectra of Zr-TUD-1 (Fig. 4) showed a weak and broad peak between 240 and 280 nm which are assigned to $O^{2-} \rightarrow Zr^{4+}$ charge transfer interactions with Zr in low coordination states. These can principally be due either to isolated Zr or to the presence of small Zr_xO_y clusters in the silica network of TUD-1 [36]. Given the fact that this spectrum is entirely different to the spectrum of commercial ZrO_2 the existence of small Zr_xO_y clusters can be ruled out. Thus the UV–vis spectra support the observation that zirconium is incorporated into the framework.

In the skeletal region of the IR spectra of a KBr pressed disc of Si-TUD-1 and Zr-TUD-1 (Fig. 5) typical bands at 1093 cm^{-1} and a shoulder at 1220 cm^{-1} due to asymmetric stretching vibrations of Si–O–Si bridges and at 798 cm^{-1} due to symmetric stretching vibration of Si–O–Si are visible. The peak at 972 cm^{-1} (Si-TUD-1) is assigned to stretching vibrations of terminal silanol groups (Si–OH) present at defect sites [36]. Additionally this peak is also assigned to Si–O–M stretching vibrations [37,38]. The presence of both of these vibra-
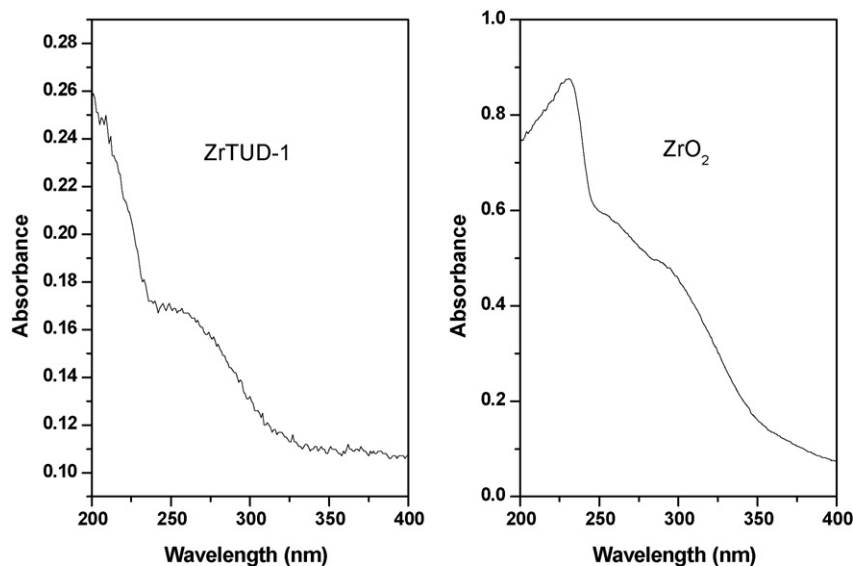
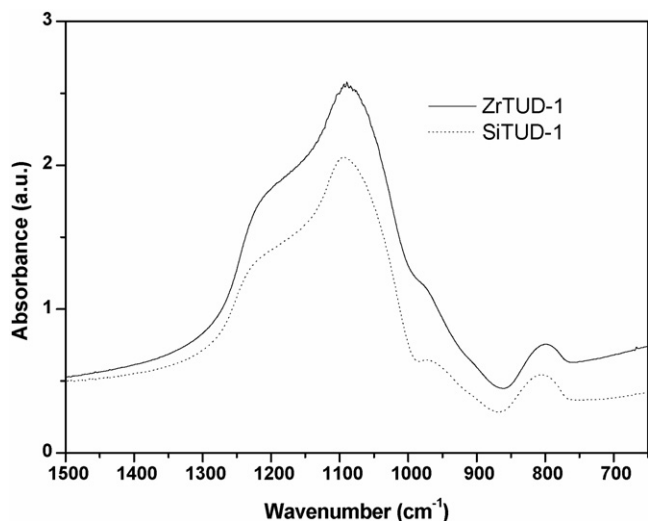Fig. 4. Diffuse reflectance UV–vis spectra of Zr-TUD-1 compared with commercial ZrO_2.

Fig. 5. FT-IR skeletal spectra of Zr-TUD-1 in comparison with all silica TUD-1 in KBr.

tions leads to a less resolved peak at 975 cm^{-1} in the case of Zr-TUD-1.

FT-IR spectra of both Si-TUD-1 and Zr-TUD-1 in the hydroxyl region (Fig. 6a) showed a band centered at 3745 cm^{-1}
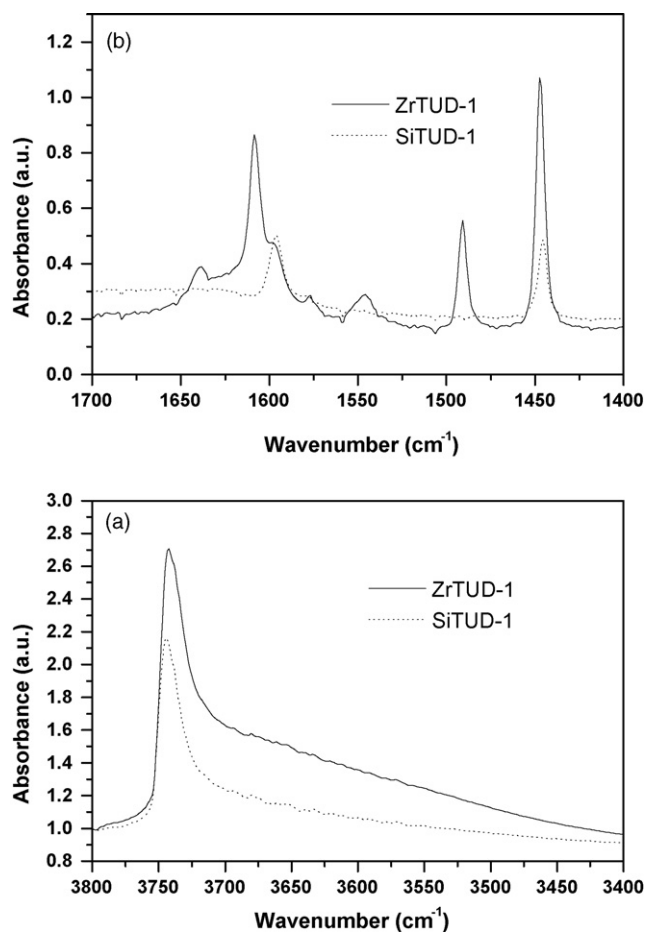

Fig. 6. FT-IR spectra of self supported wafer disc samples of Zr-TUD-1 (solid line) and Si-TUD-1 (dotted line) in: (a) hydroxyl region and (b) adsorbed pyridine at 200 °C.

that is attributed to free silanol groups. However, no band corresponding to terminal Zr–OH groups as described by Jiménez-López and co-workers was detected [34]. Although the sensitivity of these measurements are limited this is in line with zirconium that is incorporated into the framework.

FT-IR spectra of adsorbed pyridine (Fig. 6b) indicate the presence of Brønsted and Lewis acid sites. However, the Lewis acid sites necessary for the Meerwein–Ponndorf–Verley reaction are the dominant species. Thus Zr-TUD-1 combines all the characteristics for an ideal Meerwein–Ponndorf–Verley catalyst: high Lewis acidity, isolated Zr atoms, large surface area and a predictable and straightforward preparation.

3.2. Zr-TUD-1 as promising Meerwein–Ponndorf–Verley catalyst

The catalytic activity of Zr-TUD-1 was compared with Al-TUD-1 and zeolite H-beta, all with a Si/M ratio of 25 (Table 2). As expected Zr-TUD-1 shows higher activity than Al-TUD-1 in the reduction of 4-*tert*-butyl cyclohexanone (**1**), while zeolite H-beta showed the highest *cis/trans* selectivity for this substrate (entries 1, 12 and 14). As demonstrated by van Bekkum and co-workers [15,16] this is due to the narrow pore size of the zeolite in comparison to M-TUD-1. Surprisingly it is also more active than Zr-TUD-1 or Al-TUD-1. This is unexpected since both Al-free Zr-beta [18,19] and Zr-SBA-15 [23] perform better in this reaction than H-beta.

Zr-TUD-1 catalyses the reduction of acetophenone (**4**) while both Al-TUD-1 and H-beta are inactive (entries 2, 13 and 15). This is good evidence for the influence of the metal on the activity of the catalytic material. The importance of the appropriate choice of metal is also supported by the fact that Al-free Sn- and Zr-beta catalyse this reaction, too [17–19]. Similar to these catalysts Zr-TUD-1 also catalyses the reduction of **8** (entry 4) and the reduction of cinnamaldehyde (**17**). However, for the aldehydes **10** and **15** (entries 5, 6 and 8) other reactions are observed. Octanal (**10**) is not only reduced but the resulting alcohol **11** subsequently reacts with the starting material with a lower reaction rate to the symmetric acetal (**12**). When (*S*)-citronellal (**15**) was treated with Zr-TUD-1 no reduction occurred but a Prins reaction yielded (+)-isopulegol ((+)-**16**) with good selectivity. It is well known that Lewis acids catalyse this reaction; indeed it is part of the Tagasago process leading to menthol [39]. Only recently it was demonstrated that other Meerwein–Ponndorf–Verley catalysts such as H-beta, Al-free Sn-beta and in particular Al-free Zr-beta catalyse this reaction, too [40,41].

A remarkable selectivity towards the steroids oestrone (**19**) and 5α-cholestan-3-one (**21**, entries 10 and 11) was observed. The keto group on ring A of **21** was reduced almost quantitatively to yield 5α-cholestan-3-ol (**22**) with an α/β ratio of 1:6. Unlike to the reduction of **1** a clear preference for the *trans*-product is observed. This is most likely due to the steric hindrance induced by the C-19 methyl group on C-10. The keto group on ring D of oestrone (**19**), however, was no substrate for Zr-TUD-1, most likely due to steric hindrance induced by the substituents in the α-position.

Table 2
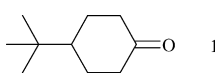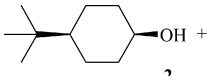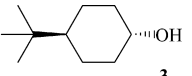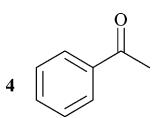Meerwein–Ponndorf–Verley-reductions catalysed by Zr-TUD-1, Al-TUD-1 and zeolite H-beta[a]
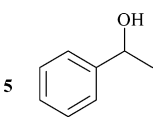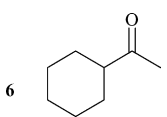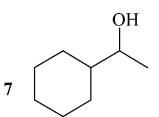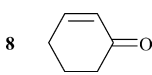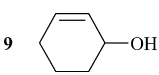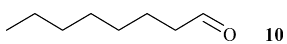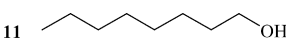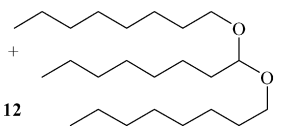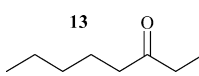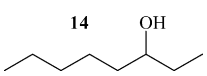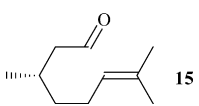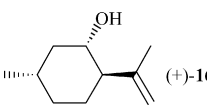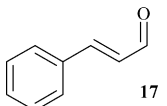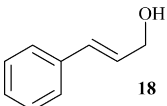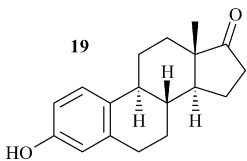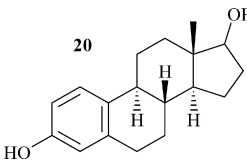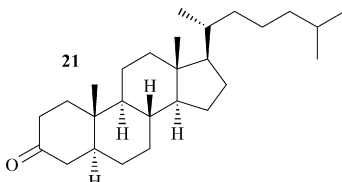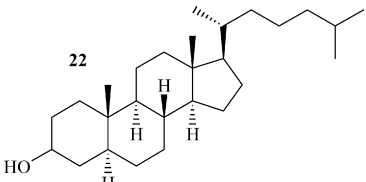
Entry	Catalyst	Substrate	Products	Conversion (%)[b]	Reaction time
1	Zr-TUD-1	**1**	**2** + **3**	95 (**2:3** = 13:2)	7 days
2	Zr-TUD-1	**4**	**5**	20	7 days
3	Zr-TUD-1	**6**	**7**	22	7 days
4	Zr-TUD-1	**8**	**9**	8	7 days
5	Zr-TUD-1	**10**	**11** + **12**	60 (**11:12** = 8:1)	4 h
6	Zr-TUD-1	**10**	**11** + **12**	85 (**11:12** = 1:4)	7 days
7	Zr-TUD-1	**13**	**14**	6	7 days
8	Zr-TUD-1	**15**	(+)-**16** + isomers	95 ((+)-**16**: isomers = 3:1)	5 days
9	Zr-TUD-1	**17**	**18**	80	5 days
10	Zr-TUD-1	**19**	**20**	0	7 days
11	Zr-TUD-1	**21**	**22**	>95 (α:β = 1:6)	7 days

Table 2 (*Continued*)

Entry	Catalyst	Substrate	Products	Conversion (%)[b]	Reaction time
12	Al-TUD-1	**1**	**2 + 3**	10 (**2**:**3** = 15:2)	7 days
13	Al-TUD-1	**4**	**5**	0	7 days
14	H-beta	**1**	**2 + 3**	99 (**2**:**3** = 19:1)	18 h
15	H-beta	**4**	**5**	0	7 days

[a] Reactions were performed with Zr-TUD-1 (Si/Zr = 25), Al-TUD-1 (Si/Al = 25) or H-beta (Si/Al = 25) (50 mg) and substrate (2 mmol) in 2-propanol (4 mL) at 80 °C for the time given.
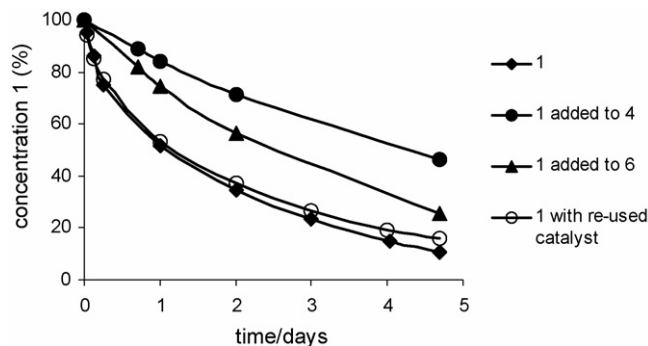
[b] Ratio of products between brackets.

Fig. 7. Zr-TUD-1 catalysed reduction of 4-*tert*-butylcyclohexanone (**1**). (♦) Conversion of **1**; (●) conversion of **1** in an equimolar mixture of **1** and **4**; (▲) conversion of **1** in an equimolar mixture of **1** and **6**; (○) conversion of **1** with Zr-TUD-1 recycled from the competition experiment with **1** and **4**.

To gain further insight into the different reactivities of Zr-TUD-1 towards the sterically not so demanding ketones **1**, **4** and **6** (entries 1, 2 and 3), the reduction of **1** was performed in the presence of equimolar amounts of **4** or **6**. Both slowed down the reduction of **1** significantly (Fig. 7), indicating that they, too, are attached to the catalyst, making it less accessible for **1**. The lower reactivity of **4** is due to conjugation, that of **6** to the sterically demanding substituent in the α-position. This is reflected by the fact that **6** has less influence on the reduction of **1** than **4**.

The addition of **4** and **6** did however, not influence the *cis/trans* ratio of the reduction of **1**. The Zr-TUD-1 was reactivated and recycled after the competition experiment with **1** and **4**. It regained virtually all of its activity upon calcination (Fig. 7), demonstrating that the catalyst remains unchanged.

4. Conclusions

The synthesis of zirconium incorporated into the three-dimensional mesoporous silicate, Zr-TUD-1, was achieved by a direct hydrothermal method using triethanolamine as template. This material was shown to possess a high surface area and acidity arising mainly from Lewis acid sites. No detectable zirconia phases were observed both in XRD and TEM. This is further supported by UV–vis and XPS studies. Zr-TUD-1 is an active, mild and recyclable catalyst in the Meerwein–Ponndorf–Verley reduction, displaying high selectivity, in particular towards the sterically demanding steroids, compounds that could not be reduced with H-beta, Al-free Sn-beta or Al-free Zr-beta.

Thus it widens the range of substrates that can be reduced with heterogeneous Meerwein–Ponndorf–Verley catalysts significantly.

References

[1] J.F. de Graauw, J.A. Peters, H. van Bekkum, J. Huskens, Synthesis (1994) 1007–1017.
[2] K. Nishide, M. Node, Chirality 14 (2002) 759–767.
[3] T. Ooi, T. Miura, Y. Itagaki, H. Ichikawa, K. Maruoka, Synthesis (2002) 279–291.
[4] Y.-C. Liu, B.-T. Ko, B.-H. Huang, C.-C. Lin, Organometallics 21 (2002) 2066–2069.
[5] E.J. Campbell, H. Zhou, S.T. Nguyen, Org. Lett. 3 (2001) 2391–2393.
[6] Y. Ishii, T. Nakano, A. Inada, Y. Kishigami, K. Sakurai, M. Ogawa, J. Org. Chem. 51 (1986) 240–242.
[7] B. Knaver, K. Krohn, Liebigs Ann. (1995) 677–683.
[8] J.L. Namy, J. Souppe, J. Collin, H.B. Kagan, J. Org. Chem. 49 (1984) 2045–2049.
[9] T. Okano, M. Matsuoka, H. Konishi, J. Kiji, Chem. Lett. (1987) 181–184.
[10] D. Klomp, K. Djanashvili, N. Cianfanelli Svennum, N. Chantapariyavat, C.-S. Wong, F. Vilela, T. Maschmeyer, J.A. Peters, U. Hanefeld, Org. Biomol. Chem. 3 (2005) 483–489.
[11] V.A. Ivanov, J. Bachelier, F. Audry, J.C. Lavalley, J. Mol. Catal. 91 (1994) 45–59.
[12] S.H. Liu, S. Jaenicke, G.K. Chuah, J. Catal. 206 (2002) 321–330.
[13] T.M. Jyothi, T. Raja, K. Sreekumar, M.B. Talawar, B.S. Rao, J. Mol. Catal. A: Chem. 157 (2000) 193–198.
[14] M.A. Aramendia, V. Borau, C. Jiménez, J.M. Marinas, J.R. Ruiz, F. Urbano, Appl. Catal. A: Gen. 249 (2003) 1–9.
[15] J.C. van der Waal, E.J. Creyghton, P.J. Kunkeler, H. van Bekkum, Top. Catal. 4 (1997) 261–268.
[16] E.J. Creyghton, S.D. Ganeshie, R.S. Downing, H. van Bekkum, J. Mol. Catal. A: Chem. 115 (1997) 457–472.
[17] A. Corma, M.E. Domine, S. Valencia, J. Catal. 215 (2003) 294–304.
[18] Y. Zhu, G. Chuah, S. Jaenicke, Chem. Commun. (2003) 2734–2735.
[19] Y. Zhu, G. Chuah, S. Jaenicke, J. Catal. 227 (2004) 1–10.
[20] Y. Zhu, G. Chuah, S. Jaenicke, J. Catal. 241 (2006) 25–33.
[21] D. Klomp, T. Maschmeyer, U. Hanefeld, J.A. Peters, Chem. Eur. J. 10 (2004) 2088–2093.

[22] R. Cohen, C.R. Graves, S.-B.T. Nguyen, J.M.L. Martin, M.A. Ratner, J. Am. Chem. Soc. 126 (2004) 14796–14803.

[23] Y. Zhu, S. Jaenicke, G.K. Chuah, J. Catal. 218 (2003) 396–404.

[24] M. Wei, K. Okabe, H. Arakawa, Y. Teraoka, Catal. Commun. 5 (2004) 597–603.

[25] J.C. Jansen, Z. Shan, L. Marchese, W. Zhou, N. van der Puil, T. Maschmeyer, J. Chem. Soc. Chem. Commun. (2001) 713–714.

[26] C. Simons, U. Hanefeld, I.W.C.E. Arends, R.A. Sheldon, T. Maschmeyer, Chem. Eur. J. 10 (2004) 5829–5835.

[27] R. Anand, M.S. Hamdy, U. Hanefeld, T. Maschmeyer, Catal. Lett. 95 (2004) 113–117.

[28] M.S. Hamdy, R. Anand, T. Maschmeyer, U. Hanefeld, J.C. Jansen, Chem. Eur. J. 12 (2006) 1782–1789.

[29] M.S. Hamdy, G. Mul, J.C. Jansen, A. Ebaid, Z. Shan, A.R. Overweg, T. Maschmeyer, Catal. Today 100 (2005) 255–260.

[30] M.S. Hamdy, G. Mul, W. Wei, R. Anand, U. Hanefeld, J.C. Jansen, J.A. Moulijn, Catal. Today 110 (2005) 264–271.

[31] Z. Shan, E. Gianotti, J.C. Jansen, J.A. Peters, L. Marchese, T. Maschmeyer, Chem. Eur. J. 7 (2001) 1437–1443.

[32] According to a calculation with HyperChem the smallest cubic box into which cholesterol fits is: 7.5 Å × 3.9 Å × 15.6 Å. The pore diameter of zeolite beta is <7.5 Å.

[33] A.B. Attygalle, S. García-Rubio, J. Ta, J. Meinwald, J. Chem. Soc. Perkin Trans. 2 (2001) 498–506.

[34] A. Infantes-Molina, J. Mérida-Robles, P. Maireles-Torres, E. Finocchio, G. Busca, E. Rodríguez-Castellón, J.L.G. Fierro, A. Jiménez-López, Microporous Mesoporous Mater. 75 (2004) 23–32.

[35] B. Rakshe, V. Ramaswamy, S.G. Hegde, R. Vetrivel, A.V. Ramasamy, Catal. Lett. 45 (1997) 41–50.

[36] E. Rodríguez-Castellón, A. Jiménez-López, P. Maireles-Torres, D.J. Jones, J. Rozière, M. Trombetta, G. Busca, M. Lenarda, L. Storaro, J. Solid State Chem. 175 (2003) 159–169.

[37] M.A. Camblor, A. Corma, J. Pérez-Pariente, J. Chem. Soc. Chem. Commun. (1993) 557–559.

[38] E. Astorino, J.B. Peri, R.J. Willey, G. Busca, J. Catal. 157 (1995) 482–500.

[39] R. Noyori, Adv. Synth. Catal. 345 (2003) 15–32.

[40] Z. Yongzhong, N. Yuntong, S. Jaenicke, G.-K. Chuah, J. Catal. 229 (2005) 404–413.

[41] Y. Nie, G.-K. Chuah, S. Jaenicke, Chem. Commun. (2006) 790–792.